



## RESEARCH LETTER

10.1002/2016GL069328

## Key Points:

- We used photoacoustic spectroscopy to study the kinetics of water uptake to aqueous particles
- We show that the mass accommodation coefficient for water condensation to liquid water exceeds 0.1
- This is outside the regime in which water uptake kinetics are expected to impact cloud formation

## Correspondence to:

J. M. Langridge,  
justin.langridge@metoffice.gov.uk

## Citation:

Langridge, J. M., M. S. Richardson, D. A. Lack, and D. M. Murphy (2016), Experimental evidence supporting the insensitivity of cloud droplet formation to the mass accommodation coefficient for condensation of water vapor to liquid water, *Geophys. Res. Lett.*, 43, 6650–6656, doi:10.1002/2016GL069328.

Received 28 APR 2016

Accepted 6 JUN 2016

Accepted article online 8 JUN 2016

Published online 28 JUN 2016

## Experimental evidence supporting the insensitivity of cloud droplet formation to the mass accommodation coefficient for condensation of water vapor to liquid water

Justin M. Langridge<sup>1</sup>, Mathews S. Richardson<sup>2,3</sup>, Daniel A. Lack<sup>2,3</sup>, and Daniel M. Murphy<sup>3</sup>

<sup>1</sup>Observation Based Research, Met Office, Exeter, UK, <sup>2</sup>Cooperative Institute for Research in Environmental Science, University of Colorado Boulder, Boulder, Colorado, USA, <sup>3</sup>Chemical Sciences Division, NOAA Earth System Research Laboratory, Boulder, Colorado, USA

**Abstract** The mass accommodation coefficient for uptake of water vapor to liquid water,  $\alpha_M$ , has been constrained using photoacoustic measurements of aqueous absorbing aerosol. Measurements performed over a range of relative humidities and pressures were compared to detailed model calculations treating coupled heat and mass transfer occurring during photoacoustic laser heating cycles. The strengths and weaknesses of this technique are very different to those for droplet growth/evaporation experiments that have typically been applied to these measurements, making this a useful complement to existing studies. Our measurements provide robust evidence that  $\alpha_M$  is greater than 0.1 for all humidities tested and greater than 0.3 for data obtained at relative humidities greater than 88% where the aerosol surface was most like pure water. These values of  $\alpha_M$  are above the threshold at which kinetic limitations are expected to impact the activation and growth of aerosol particles in warm cloud formation.

### 1. Introduction

Clouds play a key role in regulating the Earth's energy budget through interaction with solar and terrestrial radiation [Intergovernmental Panel on Climate Change (IPCC), 2013]. Liquid cloud droplets form through the activation and subsequent growth of aerosol particles [Pruppacher and Klett, 1997]. The properties of the underlying aerosol population (e.g., particle number, size, composition, and mixing state) are important in determining the resulting cloud microphysical properties, radiative properties, and lifetime [McFiggans et al., 2006]. Aerosol impacts on cloud properties are commonly referred to as indirect effects and these remain amongst the most uncertain anthropogenic drivers of climate change [IPCC, 2013].

Numerous modeling studies have demonstrated sensitivity of cloud droplet formation to the kinetics of water condensation during particle growth [Chuang, 2006; Chuang et al., 1997; Feingold and Chuang, 2002; Kulmala et al., 1996; Nenes et al., 2001]. This sensitivity arises from the impact of droplet growth rate on the maximum supersaturation that develops within a rising air parcel prior to the onset of activation [Chuang et al., 1997]. For a given aerosol population, as water uptake kinetics slow, aerosol activation is delayed, leading to higher maximum supersaturations and formation of brighter clouds containing a greater number of smaller, longer-lived cloud droplets [Kulmala et al., 1996]. Constraining the impact of water uptake kinetics on cloud formation is one step toward reducing uncertainty associated with aerosol indirect forcing of climate.

A key parameter determining the kinetics of water uptake is the mass accommodation coefficient,  $\alpha_M$ , which describes the probability that a water vapor molecule impacting a particle surface will remain within the particle [Kolb et al., 2010]. Modeling studies have shown that growth kinetics only impact cloud droplet formation significantly for  $\alpha_M < 0.1$  [Chuang et al., 1997; Raatikainen et al., 2013]. For  $\alpha_M > 0.1$ , water uptake is sufficiently fast that particle growth is limited by factors other than surface accommodation, such as diffusion of water vapor to the growing particles, and loss of heat generated during condensation.

The measurement of  $\alpha_M$  for water vapor on liquid water surfaces has been the focus of numerous experimental studies conducted over many decades. Reported values have spanned a wide range from 0.001 to 1 [Davidovits et al., 2004; Kolb et al., 2010; Miles et al., 2012; Mozurkewich, 1986]. The most recent estimates have generally converged to values above the  $\alpha_M = 0.1$  threshold for relevance to cloud droplet formation [Miles et al., 2012]. Experiments have been performed using a range of approaches. For example, droplet train

experiments have yielded  $\alpha_M$  from 0.32 to 0.17 in the temperature range 258–280 K [Li *et al.*, 2001], the cloud expansion chamber experiments of Winkler *et al.* [2006] yielded  $\alpha_M$  values close to 1 across the temperature range 250–290 K, droplet evaporation experiments conducted under vacuum by Smith *et al.* [2006] measured  $\alpha_M$  near 0.6 with little temperature dependence in the range 245–298 K, and measurements of evaporation of trapped single water droplets by Davies *et al.* [2014] derived similar values of  $\alpha_M \geq 0.5$  across the temperature range 228–293 K. In addition to experimental studies, recent theoretical work also provides evidence for there being no barrier to water accommodation ( $\alpha_M = 1$ ) [e.g., Varilly and Chandler, 2013].

In this study we present further experimental evidence showing  $\alpha_M > 0.1$  for uptake of water vapor to liquid water surfaces. This conclusion is drawn from laboratory measurements of absorption by aqueous aerosol particles conducted using photoacoustic spectroscopy. This experimental approach is distinct from all of those applied previously to this problem and is subject to different strengths and limitations. As such, our measurements provide valuable independent constraint of this important physical parameter.

## 2. Experimental

Photoacoustic spectroscopy (PAS) is increasingly being applied for the measurement of absorption by atmospheric aerosol [Arnott *et al.*, 2006; Lack *et al.*, 2012; Lewis *et al.*, 2009]. This technique measures the acoustic signal generated by absorbing aerosol exposed to intensity modulated radiation. Typically, the acoustic signal varies linearly with sample absorption strength; however, various studies have shown that this relationship breaks down in the presence of semivolatile aerosol components such as water [Arnott *et al.*, 2003; Murphy, 2009; Raspert *et al.*, 2003]. Here latent heat consumed and released during aerosol heating cycles reduces the efficiency of acoustic signal generation by reducing conductive heat transfer between the aerosol and gas phases. This leads to a low bias in photoacoustic measurements with respect to the true absorption magnitude, which from hereon shall be referred to as the PAS bias. The strength of the PAS bias depends on the extent to which evaporation and condensation occur, and it is thus sensitive to both humidity and the magnitude of  $\alpha_M$ .

Murphy [2009] developed a theoretical framework for estimating the magnitude of the PAS bias based on solving the requisite coupled heat and mass transfer equations in the transition flow regime. These equations are akin to those routinely applied to model aerosol growth in cloud formation. His work highlighted the potential for using biased photoacoustic measurements to constrain the magnitude of  $\alpha_M$ , which forms the basis for this study. There are a number of potential advantages of this approach. For example, the photoacoustic technique involves small temperature perturbations and as such near equilibrium conditions are maintained. It also employs a flow setup in which particle surfaces are continually refreshed, thus reducing susceptibility to contamination. Perhaps the most significant advantage however is that the sensitivity of the acoustic signal to  $\alpha_M$  arises from competition between heat and mass transfer as opposed to droplet growth experiments where these factors act together to limit growth rates. This results in a high sensitivity to accommodation coefficients greater than 0.1, as opposed to droplet growth measurements which are most sensitive to accommodation coefficients less than 0.1.

The laboratory setup used for experiments, its validation, and data analysis methodologies have been described in detail previously [Langridge *et al.*, 2013]. Briefly, particles were generated by atomization, dried, and size selected using a differential mobility analyzer. The particle-laden flow then passed through a home-built pressure controlled inlet, which provided active control of the downstream system pressure in the range 109–800 mb. The flow was subsequently humidified using a temperature-controlled Nafion-humidifier assembly which provided stable relative humidity (RH) control up to 90% RH. For the measurement of dry aerosol properties the humidifier assembly was bypassed. Finally, the conditioned flow passed through three measurement systems positioned in series: a photoacoustic cell (measuring particle absorption at 532 nm), a cavity ringdown cell (measuring particle extinction at 532 nm), and a condensation particle counter (measuring particle number concentration). All absorption measurements were corrected for particle number to account for (generally small) changes in particle generation efficiency during experiment runs. Particle losses between the photoacoustic cell, cavity ringdown cell, and particle counter were not accounted for based on model calculations, which predicted losses to be below 1% in the relevant particle size range (200–330 nm) [von der Weiden *et al.*, 2009]. All absorption measurements were performed at a fixed temperature of  $25 \pm 0.6^\circ\text{C}$ , achieved through active temperature control of the photoacoustic cell.

**Table 1.** Thermophysical Parameters Used for Calculation of Photoacoustic Signal Bias and Associated Uncertainties

Property	Value	Reference	Uncertainty
$c_{p,g}$ (J kg <sup>-1</sup> K <sup>-1</sup> )	$1860p_v + 1006(1 - p_v)$	Shiraiwa <i>et al.</i> [2012]	-
$L$ (J kg <sup>-1</sup> )	$3.14566 \times 10^6 - 2361.64T_\infty$	Winkler <i>et al.</i> [2006]	$\pm 1.7\%$ (Miles <i>et al.</i> [2012])
$D$ (m <sup>2</sup> s <sup>-1</sup> )	$D_{H_2O-air} \frac{pT - p_v}{pT} + D_{self} \frac{p_v}{pT}, D_{H_2O-air} = 2.178 \times 10^{-5} \left( \frac{p_0}{pT} \right) \left( \frac{T_\infty}{T_0} \right)^{1.81},$ where $D_{self} = 1.7 \times 10^{-5} \text{ m}^2 \text{ s}^{-1}$ , $pT = \text{total pressure, } p_0 = 1 \text{ atm, and } T_0 = 273.15 \text{ K.}$	Miles <i>et al.</i> [2012]	$D_{H_2O-air} \pm 7\%$ and $D_{self} -14\%/+12\%$ (Miles <i>et al.</i> [2012])
$K$ (W m <sup>-1</sup> K <sup>-1</sup> )	$\frac{K_v}{1 + 0.556 \frac{1 - p_v}{p_v}} + \frac{K_g}{1 + 1.189 \frac{1 - p_v}{p_v}}, K_v = -6.7194 \times 10^{-3} + 7.4857 \times 10^{-5} T_{\infty},$ $K_g = 3.4405 \times 10^{-3} + 7.5177 \times 10^{-5} T_{\infty}.$	Winkler <i>et al.</i> [2006]	$K_v \pm 2\%$ , $K_g \pm 2\%$ , and $K$ (additional) $\pm 1\%$ (Miles <i>et al.</i> [2012])

Experiments were performed using 200 nm dry diameter internally mixed nigrosin dye-ammonium sulphate particles (3.3:8.9 gL<sup>-1</sup>). This chemical system was chosen to meet two key criteria: absorption at the 532 nm wavelength of the photoacoustic instrument and strong equilibrium water uptake as a function of RH. In order to determine particle diameters at elevated RH, which were required to model particle absorption and the photoacoustic bias [Langridge *et al.*, 2013], the particle hygroscopicity was characterized using cavity ringdown spectroscopy. Measurements of particle extinction as a function of RH were fit to a model based on the  $\kappa$ -Kohler treatment of hygroscopic growth [Petters and Kreidenweis, 2007]. This approach derived a best fit  $\kappa$  value of 0.4 for the mixed nigrosin-ammonium sulphate particles [Langridge *et al.*, 2013], corresponding to particle water volume fractions of 0.21, 0.48, and 0.77 at RHs of 40%, 70%, and 90%, respectively. Good agreement was seen between measured data and model calculations [see Langridge *et al.*, 2013, Figure 5a] indicating the validity of the  $\kappa$ -Kohler-based approach. This figure also provides evidence that the particles remained in the liquid phase at all RHs accessed in experiments as no discontinuities in measured  $f(\text{RH})_{\text{ext}}$  associated with phase changes were observed. The importance of considering the morphology of the mixed nigrosin-ammonium sulphate-water particles for the interpretation of data is discussed further below.

Experiment runs consisted of measuring absorption as a function of RH to enable construction of humidigrams showing the change in the ratio of wet to dry particle absorption ( $f(\text{RH})_{\text{abs}}$ ) with humidity. Humidigrams were measured as a function of pressure in the range 109–800 mb. The rationale for this approach was to probe the strong pressure dependence of the PAS measurement bias, which arises from the reduced efficiency of thermal transfer from particles at low pressure. In turn, this provided a broad data set with which to evaluate  $\alpha_M$ .

### 3. Modeling

Model calculations of  $f(\text{RH})_{\text{abs}}$  including the effects of PAS bias were performed following Langridge *et al.* [2013] and Murphy [2009]. The original publications should be referenced for full details, including a detailed list of assumptions. The current application differs only by the choice of thermophysical parameters used and inclusion of associated uncertainties. The key result is that the ratio of the photoacoustic signal recorded under wet and dry conditions ( $S_{\text{ratio}}$ ) is given by

$$S_{\text{ratio}} = \frac{|\beta_T - i\omega\tau|}{|\beta_T(1 + f_M) - i\omega\tau|} \left( 1 + f_M \frac{T_\infty c_{p,g}}{L} \right) \text{ with } f_M = \frac{\beta_M}{\beta_T} \frac{LDp_v M_v}{KRT_\infty^2} \left( \frac{LM_v}{RT_\infty} - 1 \right) \text{ and } \tau = \frac{r_0^2 \rho_a c_a}{3K}, \quad (1)$$

where  $\beta_T$  and  $\beta_M$  are the thermal and mass transition flow correction factors which are dependent upon Knudsen number and the thermal/mass accommodation coefficient [Winkler *et al.*, 2006],  $\omega$  is the laser modulation frequency (Hz),  $T_\infty$  ambient temperature (298 K),  $c_{p,g}$  specific heat of the bath gas at constant pressure (Table 1),  $L$  latent heat of evaporation (Table 1),  $D$  diffusion coefficient of water in humid air (Table 1),  $p_v$  partial pressure of water vapor,  $M_v$  molecular weight of water (0.018 kg mol<sup>-1</sup>),  $R$  universal gas constant (8.3144 J K<sup>-1</sup> mol<sup>-1</sup>),  $K$  thermal conductivity of humid air (Table 1),  $r_0$  particle radius,  $\rho_a$  particle density, and  $c_a$  particle specific heat (4148 J kg<sup>-1</sup> K<sup>-1</sup>). Calculations were performed using a number of  $\alpha_M$  values spanning the range 0.05 to 1.

The uncertainty in model calculations arising from uncertainty in input thermophysical quantities  $L$ ,  $D$ , and  $K$  was evaluated by explicitly propagating uncertainty in these parameters through equation (1) to provide the

maximum range in  $S_{\text{ratio}}$  possible. Table 1 gives the uncertainty values used. An additional uncertainty in model calculations was introduced from the assumption of pure water droplets, which for the aqueous nigrosin-ammonium sulphate particles used in experiments was not valid, particularly at low RH. To probe sensitivity to this limitation, two sets of model calculations were performed which provided bounds on the expected PAS bias. The first set (“no mixing” case) assumed that particles took up water without any mixing into the particle bulk. Beyond  $\text{RH} \approx 12\%$  (corresponding to approximately five monolayers of water on the particle surface), these calculations were identical to those for a pure water surface. The second set of calculations (“homogeneous mixing” case) applied the PAS evaporation bias only to the particle volume fraction corresponding to water. Here the water volume fraction was used as a proxy for the particle surface water coverage and this approach was essentially equivalent to assuming instantaneous homogeneous mixing of water following uptake. We have not considered a case whereby nigrosin was surface active and thus acted to limit the particle surface water coverage below that predicted by the homogeneous mixing case. While we do not have evidence to rule out this possibility, we note that it would not change the overriding interpretation of measurement data, as described further in section 4.

#### 4. Results

Figure 1 shows the ratio of the humidified to dry photoacoustic absorption signal measured at pressures of 109, 200, 300, 400, and 800 mb (solid circles). Figure 1 (left column) compares measurements to model calculations performed for the no mixing case. Figure 1 (right column) compares the same data to model calculations performed assuming instantaneous homogeneous mixing of water.

At all humidities and pressures the measured PAS absorption is strongly low biased. The largest bias (calculated as the ratio of the measured absorption to that calculated for the case of no evaporation) is approximately 0.2. The magnitude of the PAS bias increases with humidity, as expected from the dependence of the mass flux on the partial pressure of water vapor [Murphy, 2009]. In addition, the bias increases with decreasing pressure, as expected from the lower thermal conductivity of air which reduces the efficiency of heat transfer from heated particles, making the mass transfer pathway more competitive.

In all cases a single set of model results does not reproduce the experimental data well. For calculations performed assuming no mixing (pure water surfaces), all experimental data are bound by calculations with  $\alpha_M$  in the range 0.1–1. The functional forms of the model calculations do not represent the measured data well, as evidenced by the experimental data cutting across model curves calculated for different values of  $\alpha_M$ . This behavior suggests that the magnitude of the measured PAS bias was limited by the particle surface water availability and that the assumption of a pure water surface was not valid, particularly at low RH. Despite this limitation, comparing model and experimental data for this case does provide bounds on the possible value of  $\alpha_M$ . For  $\alpha_M < 0.1$ , calculations cannot reproduce the observed PAS bias, thus providing an absolute lower limit on the value  $\alpha_M$ . For the highest RH measurements ( $\text{RH} > 88\%$ ), where the particle water volume fraction was approximately 77% and the assumption of a pure water surface most valid, measurements are consistent with  $\alpha_M > 0.3$ .

For calculations performed assuming homogeneous mixing, the quantitative agreement with measurements is poorer. The modeled bias underestimates measured values, even for simulations performed at the kinetic limit with  $\alpha_M = 1$ . However, the qualitative shape of the modeled curves better matches observations than those for the no mixing (pure water) case. This suggests that although mixing of water into the particle bulk may not be as extensive as predicted by instantaneous homogeneous mixing, the impact of limited particle water availability was impacting the magnitude of the measured PAS bias, particularly at low RH. Agreement between measured and modeled data for this case is markedly worse at low pressure, which is discussed further below.

To explore the relationship between particle surface water coverage and the observed PAS bias, we inverted measurement data to derive the effective water surface coverage needed to yield consistency between model and measured data for two assumed values of  $\alpha_M$ : 0.1 and 1. The inversion was performed by assuming that the PAS signal bias applied only to the fraction of the particle surface covered by water.

Figure 2 shows results of this inversion and includes the theoretical surface coverages calculated for both the no mixing and homogeneous mixing cases. Inversions performed using  $\alpha_M = 1$  show surface coverages that are well bound by theoretical predictions for the two idealized mixing cases, with good consistency between

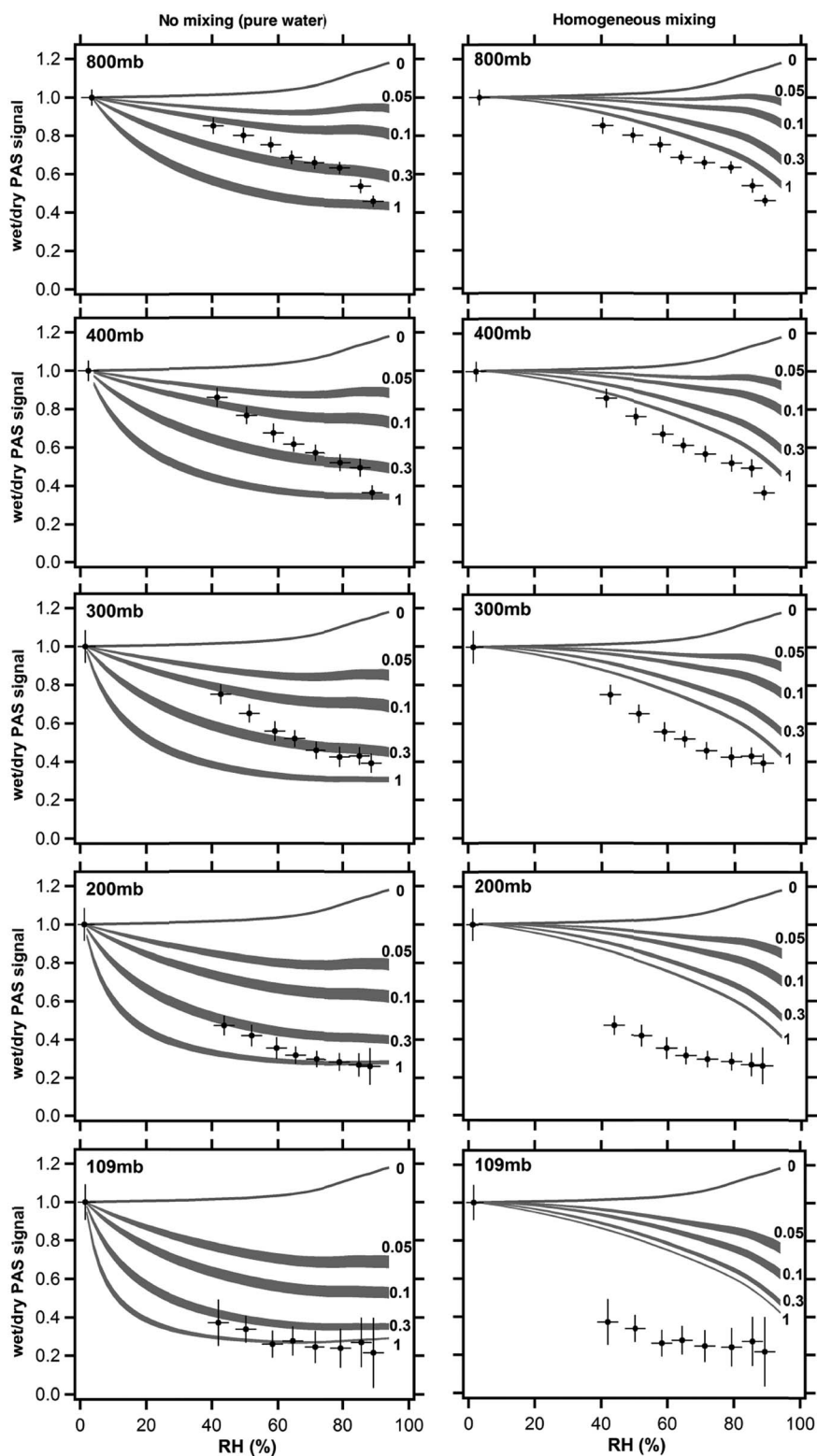


**Figure 1.** Ratio of wet to dry photoacoustic absorption measured for 200 nm dry diameter aqueous nigrosin-ammonium sulphate particles (solid circles). Left column: Comparison to model calculations ( $\alpha_M$  in range 0–1) assuming no mixing of water into the particle bulk. Right column: Comparison to calculations assuming instantaneous homogeneous mixing of water within the particles. Experimental data points are 90 s means with the y axis error bars denoting the  $1\sigma$  precision, which dominated the total measurement uncertainty. The x axis error bars show the absolute error in the RH measurements ( $\pm 3\%$ ). Each of the model curves is a shaded region indicating the uncertainty range determined as described in the main text.

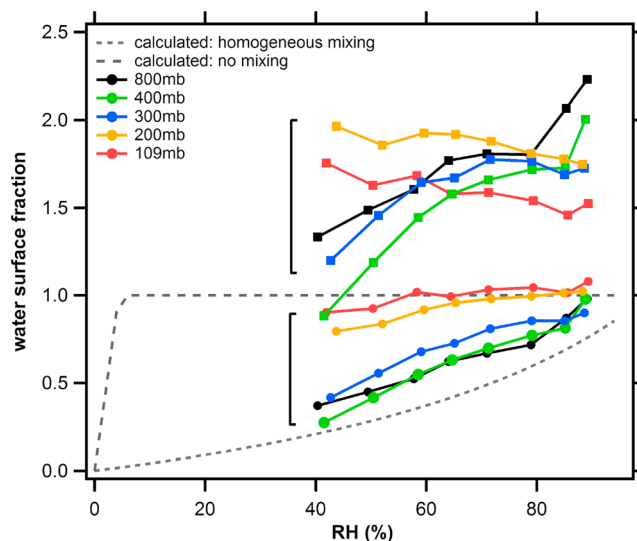


**Figure 2.** Particle surface water coverage calculated from biased photoacoustic measurements assuming  $\alpha_M = 1$  (circles) and  $\alpha_M = 0.1$  (squares). Also included are the surface water coverages calculated under idealized assumptions of no mixing and instantaneous homogeneous mixing of water into the particle bulk following uptake.

predictions from measurements at 800, 400, and 300 mb. These measurements suggest that there was significant mixing of water into the particle bulk, with the absolute water surface coverage enhanced with respect to the instantaneous homogeneous mixing case by approximately 0.17 (see Figure 2). The predicted surface coverage from measurements at the lowest pressures of 109 and 200 mb are not consistent with this interpretation and show better agreement with the no mixing case. If particle mixing state is independent of ambient pressure then this result is hard to reconcile and may indicate limitations in our calculation of  $S_{\text{ratio}}$  at low pressure. In particular, calculations assume that water vapor is a trace species. At the lowest pressure of 109 mb, water vapor represents 26% of all gas phase molecules at 90% RH and thus the validity of this assumption is no

longer clear [Miles et al., 2012]. Similar inversions performed using  $\alpha_M = 0.1$  show that measurements can only be reconciled with model calculations using water surface coverages greater than 1, which is not physically possible. This demonstrates that despite complications associated with particle morphology and composition, our measurements provide robust evidence for  $\alpha_M > 0.1$ .

We note that the potential case whereby nigrosin was surface active, and thereby limited particle surface water coverage below that predicted for the homogeneous mixing case has not been considered. While we cannot rule this behavior out, by limiting surface water coverage it would serve to reduce the magnitude of the modeled PAS bias with respect to the homogeneous mixing case and thus further increase discrepancy between modeled and observed behavior. Thus, should nigrosin have been acting as a surfactant, it would serve only to further support the conclusion that  $\alpha_M > 0.1$ .

## 5. Conclusion

Photoacoustic measurements of aqueous nigrosin-ammonium sulphate aerosol have been used to constrain the mass accommodation coefficient for uptake of water vapor to liquid water,  $\alpha_M$ . Measurements performed over a range of relative humidities and pressures were compared to detailed model calculations treating coupled heat and mass transfer occurring during photoacoustic laser heating cycles. Our measurements provide strong evidence that  $\alpha_M$  is greater than 0.1; a conclusion that was shown to be robust despite uncertainties in the morphology of the mixed-component particles studied. This result adds to a growing body of evidence suggesting that  $\alpha_M > 0.1$  and therefore above the threshold at which kinetic limitations are expected to impact the activation and growth of aerosol particles in warm cloud formation. This work has brought to bear a unique experimental approach with different strengths and limitations to those applied previously to measure  $\alpha_M$  and as such provides a useful independent result. While the focus of our study has been  $\alpha_M$  for uptake of water vapor to pure water surfaces, various studies have suggested potential for depressed droplet growth rates for real-world aerosol due to additional factors such as the presence of film-forming compounds [Feingold and Chuang, 2002], slow solute dissolution [Asa-Awuku and Nenes, 2007], and viscous glass-like aerosol phases [Bones et al., 2012]. Evidence from field measurements has recently emerged showing that despite these mechanisms,  $\alpha_M > 0.1$  is also routinely observed for ambient particles across a range of environments [Raatikainen et al., 2013]. Further measurements corroborating this result are needed to fully resolve this long standing question in cloud physics research.

### Acknowledgments

We would like to thank Chuck Brock for assistance in setting up aerosol generation and sizing equipment and for numerous useful discussions related to this work. This work was supported through NOAA climate funding. The experimental data needed to reproduce article figures are available from the authors upon request (justin.langridge@metoffice.gov.uk).

### References

- Arnott, W. P., H. Moosmuller, P. J. Sheridan, J. A. Ogren, R. Raspet, W. V. Slaton, J. L. Hand, S. M. Kreidenweis, and J. L. Collett (2003), Photoacoustic and filter-based ambient aerosol light absorption measurements: Instrument comparisons and the role of relative humidity, *J. Geophys. Res.*, *108*(D1), 4034, doi:10.1029/2002JD002165.
- Arnott, W. P., J. W. Walker, H. Moosmuller, R. A. Elleman, H. H. Jonsson, G. Buzorius, W. C. Conant, R. C. Flagan, and J. H. Seinfeld (2006), Photoacoustic insight for aerosol light absorption aloft from meteorological aircraft and comparison with particle soot absorption photometer measurements: DOE Southern Great Plains climate research facility and the coastal stratocumulus imposed perturbation experiments, *J. Geophys. Res.*, *111*, D05502, doi:10.1029/2005JD005964.
- Asa-Awuku, A., and A. Nenes (2007), Effect of solute dissolution kinetics on cloud droplet formation: Extended Kohler theory, *J. Geophys. Res.*, *112*, D22201, doi:10.1029/2005JD006934.
- Bones, D. L., J. P. Reid, D. M. Lienhard, and U. K. Krieger (2012), Comparing the mechanism of water condensation and evaporation in glassy aerosol, *Proc. Natl. Acad. Sci. U.S.A.*, *109*(29), 11,613–11,618.
- Chuang, P. Y. (2006), Sensitivity of cloud condensation nuclei activation processes to kinetic parameters, *J. Geophys. Res.*, *111*, D09201, doi:10.1029/2005JD006529.
- Chuang, P. Y., R. J. Charlson, and J. H. Seinfeld (1997), Kinetic limitations on droplet formation in clouds, *Nature*, *390*(6660), 594–596.
- Davidovits, P., et al. (2004), Mass accommodation coefficient of water vapor on liquid water, *Geophys. Res. Lett.*, *31*, L22111, doi:10.1029/2004GL020835.
- Davies, J. F., R. E. H. Miles, A. E. Haddrell, and J. P. Reid (2014), Temperature dependence of the vapor pressure and evaporation coefficient of supercooled water, *J. Geophys. Res. Atmos.*, *119*, 10,931–10,940, doi:10.1002/2014JD022093.
- Feingold, G., and P. Y. Chuang (2002), Analysis of the influence of film-forming compounds on droplet growth: Implications for cloud microphysical processes and climate, *J. Atmos. Sci.*, *59*(12), 2006–2018.
- Intergovernmental Panel on Climate Change (IPCC) (2013), Climate Change 2013: The Physical Science Basis, in *Contribution of Working Group I to the Fifth Assessment Report of the Intergovernmental Panel on Climate Change*, edited by T. F. Stocker et al., pp. 1535, Cambridge Univ. Press, Cambridge, U. K., and New York.
- Kolb, C. E., et al. (2010), An overview of current issues in the uptake of atmospheric trace gases by aerosols and clouds, *Atmos. Chem. Phys.*, *10*(21), 10,561–10,605.
- Kulmala, M., P. Korhonen, T. Vesala, H. C. Hansson, K. Noone, and B. Svenningsson (1996), The effect of hygroscopicity on cloud droplet formation, *Tellus, Ser. B*, *48*(3), 347–360.
- Lack, D. A., M. S. Richardson, D. Law, J. M. Langridge, C. D. Cappa, R. J. McLaughlin, and D. M. Murphy (2012), Aircraft instrument for comprehensive characterization of aerosol optical properties, Part 2: Black and brown carbon absorption and absorption enhancement measured with photo acoustic spectroscopy, *Aerosol Sci. Technol.*, *46*(5), 555–568.
- Langridge, J. M., M. S. Richardson, D. A. Lack, C. A. Brock, and D. M. Murphy (2013), Limitations of the photoacoustic technique for aerosol absorption measurement at high relative humidity, *Aerosol Sci. Technol.*, *47*(11), 1163–1173.
- Lewis, K. A., et al. (2009), Reduction in biomass burning aerosol light absorption upon humidification: Roles of inorganically-induced hygroscopicity, particle collapse, and photoacoustic heat and mass transfer, *Atmos. Chem. Phys.*, *9*(22), 8949–8966.
- Li, Y. Q., P. Davidovits, Q. Shi, J. T. Jayne, C. E. Kolb, and D. R. Worsnop (2001), Mass and thermal accommodation coefficients of H<sub>2</sub>O(g) on liquid water as a function of temperature, *J. Phys. Chem. A*, *105*(47), 10,627–10,634.
- McFiggans, G., et al. (2006), The effect of physical and chemical aerosol properties on warm cloud droplet activation, *Atmos. Chem. Phys.*, *6*, 2593–2649.
- Miles, R. E. H., J. P. Reid, and I. Riipinen (2012), Comparison of approaches for measuring the mass accommodation coefficient for the condensation of water and sensitivities to uncertainties in thermophysical properties, *J. Phys. Chem. A*, *116*(44), 10,810–10,825.
- Mozurkewich, M. (1986), Aerosol growth and the condensation coefficient for water—A review, *Aerosol Sci. Technol.*, *5*(2), 223–236.
- Murphy, D. M. (2009), The effect of water evaporation on photoacoustic signals in transition and molecular flow, *Aerosol Sci. Technol.*, *43*(4), 356–363.
- Nenes, A., S. Ghan, H. Abdul-Razzak, P. Y. Chuang, and J. H. Seinfeld (2001), Kinetic limitations on cloud droplet formation and impact on cloud albedo, *Tellus, Ser. B*, *53*(2), 133–149.
- Petters, M. D., and S. M. Kreidenweis (2007), A single parameter representation of hygroscopic growth and cloud condensation nucleus activity, *Atmos. Chem. Phys.*, *7*(8), 1961–1971.
- Pruppacher, H. R., and J. D. Klett (1997), *Microphysics of Clouds and Precipitation*, 2nd ed., Kluwer Acad., Dordrecht, Netherlands.
- Raatikainen, T., et al. (2013), Worldwide data sets constrain the water vapor uptake coefficient in cloud formation, *Proc. Natl. Acad. Sci. U.S.A.*, *110*(10), 3760–3764.
- Raspet, R., W. V. Slaton, W. P. Arnott, and H. Moosmuller (2003), Evaporation-condensation effects on resonant photoacoustics of volatile aerosols, *J. Atmos. Oceanic Technol.*, *20*(5), 685–695.
- Shiraiwa, M., C. Pfrang, T. Koop, and U. Poschl (2012), Kinetic multi-layer model of gas-particle interactions in aerosols and clouds (KM-GAP): Linking condensation, evaporation and chemical reactions of organics, oxidants and water, *Atmos. Chem. Phys.*, *12*(5), 2777–2794.
- Smith, J. D., C. D. Cappa, W. S. Drisdell, R. C. Cohen, and R. J. Saykally (2006), Raman thermometry measurements of free evaporation from liquid water droplets, *J. Am. Chem. Soc.*, *128*(39), 12,892–12,898.
- Varilly, P., and D. Chandler (2013), Water evaporation: A transition path sampling study, *J. Phys. Chem. B*, *117*(5), 1419–1428.
- von der Weiden, S. L., F. Drewnick, and S. Borrmann (2009), Particle Loss Calculator—A new software tool for the assessment of the performance of aerosol inlet systems, *Atmos. Meas. Tech.*, *2*(2), 479–494.
- Winkler, P. M., A. Vrtala, R. Rudolf, P. E. Wagner, I. Riipinen, T. Vesala, K. E. J. Lehtinen, Y. Viisanen, and M. Kulmala (2006), Condensation of water vapor: Experimental determination of mass and thermal accommodation coefficients, *J. Geophys. Res.*, *111*, D19202, doi:10.1029/2006JD007194.